ELSEVIER

Biochimica et Biophysica Acta 1368 (1998) 343–354

BIOCHIMICA ET BIOPHYSICA ACTA
BBA

Studies of kinetics and equilibrium membrane binding of class A and class L model amphipathic peptides [1]

I.V. Polozov [a], A.I. Polozova [a], V.K. Mishra [b], G.M. Anantharamaiah [b], J.P. Segrest [b], R.M. Epand [a,*]

[a] *Department of Biochemistry, McMaster University Health Sciences Center, 1200 Main St. West, Hamilton, Ontario L8N 3Z5, Canada*
[b] *Departments of Medicine and Biochemistry and the Atherosclerosis Research Unit, University of Alabama Medical Center, Birmingham, AL 35294, USA*

Received 13 May 1997; revised 26 August 1997; accepted 26 August 1997

Abstract

We studied the kinetics and equilibrium membrane binding of two amphipathic α-helical peptides: the 18L peptide, which belongs to the class L (lytic peptides), and the Ac-18A-NH_2 peptide of the class A (apolipoprotein), according to classification of Segrest et al. ((1990) Proteins, 8, 103–117). Both for cationic 18L and zwitterionic Ac-18A-NH_2, the presence of acidic lipids increased the membrane binding constants by two orders of magnitude. The free energy of peptide–membrane association was in the range of 8.5–12.8 kcal/mol. Binding isotherms corresponded to monomer partitioning with saturation at high peptide/lipid ratios. This was also supported by stopped flow studies of the kinetics of peptide-membrane association as measured by peptide tryptophan fluorescence or by energy transfer from the peptide to the lipid-anchored anthrylvinyl fluorophor. The apparent time required for peptide–membrane equilibration was in the millisecond range. At low peptide/lipid ratios it depended on lipid concentration and was independent of the peptide concentration. The rate of peptide–membrane association was found to be relatively close to the diffusion limit. Thus peptide–membrane affinity was mostly determined by the peptide dissociation rate, i.e. higher membrane affinity correlated with a decrease in dissociation rate and with a slower peptide exchange. We have shown that the dynamic character of the

Abbreviations: 18L, GIKKFLGSIWKFIKAFVG; Ac-18A-NH_2, *N*-Acetyl-DWLKAFYDKVAEKLKEAF-amide; DOPC, dioleoylphosphatidylcholine; DOPE, dioleoylphosphatidylethanolamine; DOPG, dioleoylphosphatidylglycerol; DMPC, dimyristoylphosphatidylcholine; ANTS, aminonaphthalene-3,6,8-trisulfonic acid; DPX, *p*-xylenebis-(pyridinium bromide); LUV, large unilamellar vesicles; MLV, multilamellar lipid vesicles; P_f, the peptide concentration in water; P_b, the peptide concentration in the membrane; P_0, total peptide concentration; L, lipid concentration; K, the equilibrium peptide-membrane binding constant; ΔG_b, the free energy of peptide–membrane binding; r, bound peptide/lipid ratio; k_a, the rate constant of peptide–membrane association; k_d, the rate constant of peptide–membrane dissociation; P_{be}, the equilibrium amount of peptide bound to the membrane; R, the observed rate constant for peptide–membrane binding

* Corresponding author. Fax: +1 (905) 522-9033; E-mail: epand@fhs.mcmaster.ca

[1] This work was supported by the Medical Research Council of Canada, grant MT-7654 and in part by NIH 90734343.

PII S0005-2736(97)00210-1

peptide membrane equilibrium can be used for selective peptide targeting and disruption of membranes with a specific lipid composition.

Keywords: Membrane partitioning; Lytic peptide; Apolipoprotein; Stopped flow; Tryptophan fluorescence

1. Introduction

Lipid–peptide interactions are known to play a key role in many biological phenomena. Interactions of peptides with membranes also provide a model system for aspects of lipid–protein interactions. Many membrane-active peptides have an important common structural feature, they can potentially form an amphipathic α-helix. Such an α-helix has opposing hydrophilic and hydrophobic faces oriented along the long axis of the helix (for a general discussion see [1]). While there have appeared a number of works on peptide–membrane interactions (reviews [2,3]), there have been relatively few systematic studies of lipid effects on membrane binding properties of amphipathic α-helical peptides. Even less papers deal with the dynamic character of peptide binding [4–9,19]. Membrane binding is the first step in peptide–membrane interactions. Thus characterization of the peptide–membrane binding is a prerequisite for the study of all other aspects of peptide–membrane interactions. In this paper we describe systematic studies of the kinetics and equilibrium membrane binding of two amphipathic α-helical peptides: the cationic 18L peptide which belongs to class L (lytic) and the zwitterionic Ac-18A-NH_2 peptide belonging to class A (apolipoprotein), according to the classification of Segrest et al. [10]. It has been found previously that class A and class L peptide analogs have an opposing activity on a number of biological phenomena such as erythrocyte lysis or neutrophil activation [11]. We recently studied modulation of membrane effects of 18L and Ac-18A-NH_2 peptides by the lipid composition [12] and found that fusion and leakage caused by these peptides are modulated strongly by membrane non-bilayer phase propensity and by the presence of acidic lipids. Peptides were able to induce lateral segregation of lipids in binary systems of zwitterionic and acidic lipids [13]. Here we studied if the same factors can affect peptide membrane affinity and the dynamic character of the peptide–membrane equilibrium. We also tested if the opposing activities of class A and class L result from membrane binding.

2. Materials and methods

2.1. Materials

Details of the synthesis and characterization of the peptides have been described elsewhere [11,14]. Peptides were synthesised by the solid phase method using t-BOC chemistry. Peptides were cleaved from the resin using anhydrous HF and purified by reverse phase HPLC [15]. The following peptides were used in the work: 18L, GIKKFLGSIWKFIKAFVG [11]; Ac-18A-NH_2, *N*-Acetyl-DWLKAFYDKVAEKL-KEAF-amide [14,16].

DOPC, DOPE, DMPG, DOPG were purchased from Avanti Polar Lipids (Alabaster, AL) and were used without further purification. Aminonaphthalene-3,6,8-trisulfonic acid (ANTS), *p*-xylenebis-(pyridinium bromide) (DPX) were obtained from Molecular Probes (Eugene, OR). Spectroscopy grade Lubrol PX was purchased from Calbiochem (San Diego, CA). All other reagents were of analytical grade. Buffers were prepared in double distilled deionized water.

2.2. Liposome preparation

Multilamellar vesicles (MLV) were made from vacuum dried lipid films by suspending them in an appropriate buffer (20 mM Tris–HCl, 1 mM EDTA, 0.02% NaN_3, pH 7.4, unless otherwise stated) followed by shaking and less than 20 s of low power sonication. Large unilamellar vesicles were made by multiple extrusion of MLV through two stacked 100 nm pore polycarbonate filters (Nucleopore Corp., Pleasanton, CA). Lipid concentration of the vesicles was determined using a phosphate assay [17].

2.3. Tryptophan fluorescence

Changes in peptide tryptophan fluorescence were used to monitor association of peptides with membranes. The spectra were recorded in the range of

310–480 nm with excitation at 280 nm and bandwidths of 4 nm for both excitation and emission. Excitation at 280 nm was chosen to reduce overlap with the Raman scattering peak from water. Fluorescence experiments were done on an SLM-Aminco AB-2 Luminescence spectrophotometer (Urbana, IL). Unless otherwise stated, measurements were done in 3 ml quartz cuvettes with stirring and thermostating at 25°C.

2.4. Kinetics of peptide binding to liposomes

The time course of binding was monitored by the increase in peptide tryptophan fluorescence at 330 nm upon membrane binding. Fluorescence was measured using a stopped-flow accessory for the SLM-Aminco AB-2, with a time resolution of up to 1 ms, and a time delay of 2 ms. To improve the signal-to-noise ratio we averaged at least five consecutive runs. Fluorescence was measured at excitation and emission wavelengths of 280 and 330 nm, respectively, and 4 and 8 nm slits.

2.5. Leakage of aqueous content

The ANTS/DPX assay [18,20], dequenching of ANTS released into the medium, was used to monitor leakage induced by peptide interaction with vesicles. Multilamellar vesicles (MLV) were made in buffer (20 mM Tris–HCl, 1 mM EDTA, 0.02% NaN_3, pH 7.4) containing 12.5 mM ANTS and 45 mM DPX. The pH of the buffer was adjusted after dissolution of ANTS and DPX. LUV were prepared by extrusion and separated from nonencapsulated media by passage through a Sephadex G-75 column equilibrated with buffer containing 25 mM NaCl for osmotic strength compensation. Leakage was monitored by following the increase of fluorescence intensity at 530 nm using 360 nm excitation and bandwidths of 2 and 16 nm for excitation and emission, respectively. A UV bandpass filter was used on the excitation side, and a 390 nm cut-off filter on the emission side were used to diminish scattered light. 0% leakage was assigned to ANTS fluorescence immediately after mixing peptide solution and vesicles suspension. The 100% leakage level was determined by vesicle disruption after the addition of 50 μl of 10% Lubrol PX. Fluorescence increase from background to 100% leakage was more than 10-fold.

3. Results

Fluorescence spectra of the peptides, Ac-18A-NH_2 and 18L, in water were found to be the same with a fluorescence maximum at 351 nm. The total intensity of fluorescence was found to be proportional to peptide concentration up to 200 μM, and higher if corrected for inner filter effects both in water and in methanol (data not shown). This is indicative that these peptides do not undergo aggregation in this range of concentration and exist as monomers in water as well as in methanol. This is consistent with the previous CD studies of Ac-18A-NH_2 which showed that the peptide in buffer exists essentially as a random coil [14].

3.1. Equilibrium binding studies

Binding of peptides to membranes is accompanied by a blue shift of tryptophan fluorescence emission. The spectra of membrane-bound peptides were found to be shifted to the blue compared with the peptides dissolved in *n*-octanol or ethyl acetate. Fluorescence spectra of 18L and Ac-18A-NH_2 peptides coincided in organic solvents, thus only 18L spectra are shown on Fig. 1. Both 18L and Ac-18A-NH_2 peptides are poorly soluble in more hydrophobic solvents, thus it was difficult to evaluate the exact hydrophobicity of the membrane environment of the peptide tryptophan. However, it can be concluded that it is quite hydrophobic.

Previously membrane binding constants have been estimated from the half-shift of the tryptophan emission spectrum [21,22] or from the increase of fluorescence intensity at fixed wavelength [23,24]. We found intensity changes at one particular wavelength susceptible to large error. In addition, the fluorescence of peptides with a high affinity for membranes may be self quenched at a high peptide/lipid ratio as a consequence of peptide association in the membrane. We suggest quantitating the binding from the deconvolution of the spectra into membrane-bound and free components. Peptide–membrane association *a priori* is not a one step process, as a number of peptide

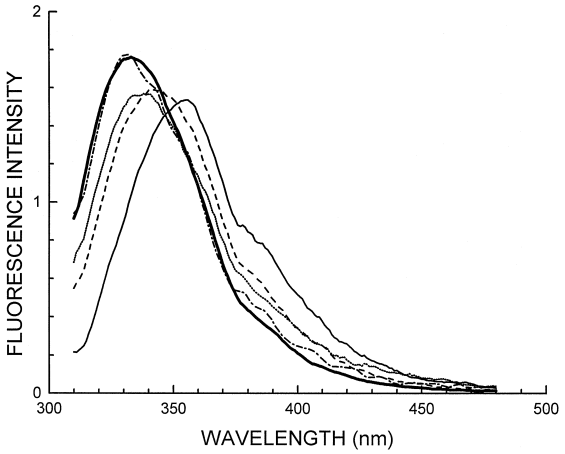

Fig. 1. Tryptophan fluorescence spectra of peptide 18L in solvents and in membrane environment (DOPC:DOPE, 1:1). Spectra scaled to the same integral intensity. Fluorescence background subtracted. Bold solid line – spectrum of 18L in membrane environment, solid line – 18L in water, dashed line – 18L in ethanol, dotted line – 18L in octyl alcohol, dash-dotted line – 18L in hexane, spectrum in hexane had much less intensity due to poor peptide solubility.

arrangements within the bilayer are possible. It is not straightforward how these different arrangements would affect the fluorescence spectrum of tryptophan. However, our data support the idea that at a relatively low peptide/lipid ratio there exist only one bound state corresponding to the most blue-shifted tryptophan fluorescence spectrum. In the course of the titration of the peptide solution with liposomes (for typical titration experiment, see Fig. 2) a final intensity increase and fluorescence shift are obtained. A further increase in liposome concentration did not give any additional change, after background subtraction. At very high lipid concentration, a decrease in fluorescence intensity, due to a scattering effect, was observed without a shift in the wavelength of maximal emission. The same reproducible blue-shifted shape of the tryptophan spectra was observed in the experiments on the titration of LUV (at sufficiently high lipid concentration) with peptides. In these experiments, tryptophan fluorescence intensity was linear with peptide concentration and after background subtraction the shape of the spectrum was independent of the peptide concentration, provided that the peptide/lipid ratio was sufficiently low. We found that for every particular peptide and lipid system, the shape of the membrane-bound peptide spectrum was different, although reproducible. Spectra of 18L bound to membranes were generally more blue-shifted than those of Ac-18A-NH_2 under identical conditions. The tryptophan environment of peptides bound to membranes containing acidic lipids was less hydrophobic than it was in zwitterionic membranes.

Knowledge of the peptide tryptophan spectrum, both in solution and in the membrane bound state, makes it possible to determine the peptide distribution between aqueous and membrane environments. Each spectrum in the course of the titration can be fitted by the superposition of the spectrum of the membrane-bound and of the free peptide (Fig. 2, inset). That is, in the course of the titration of peptide of concentration P_0, for every lipid concentration L, the fluorescence intensity at a particular wavelength λ, $I_\lambda(L)$, can be represented as:

$$I_\lambda(L) = P_f(L) \cdot I_{\lambda 0} + P_b(L) \cdot I_{\lambda\infty}$$

where

$$P_0 = P_f(L) + P_b(L) \text{ for all } L$$

$I_{\lambda 0}$ and $I_{\lambda\infty}$ are the specific intensities for the peptide in water and in membrane respectively, at wavelength λ. $P_f(L)$ and $P_b(L)$ are the peptide concentrations in water and in membrane. For every L value, $P_f(L)$ and $P_b(L)$ can be found numerically by least square optimisation. The standard deviation between the experimental points and the curve fit was comparable to the deviation between consecutive spectra of the same sample and usually was within 2%, but was higher (5%) when close to the sensitivity limit of the technique at low peptide concentrations. Knowledge of the amounts of bound and free peptide at every lipid concentration makes it possible to reconstruct binding isotherms ($r(P_f)$), i.e., a plot of bound peptide/lipid ratio ($r = P_b/L$) versus free peptide concentration P_f. This approach allows for the quantitative analysis, not only the titration of peptide by liposomes, but also the titration of liposomes with peptide, as well as a dilution assay [22] where binding is determined by the red shift of peptide fluorescence in a series of dilutions of peptide–liposome mixtures. The description of binding was considered valid if the binding isotherms, derived by titration of peptide with LUV or of LUV with peptide, from several concentrations, coincided.

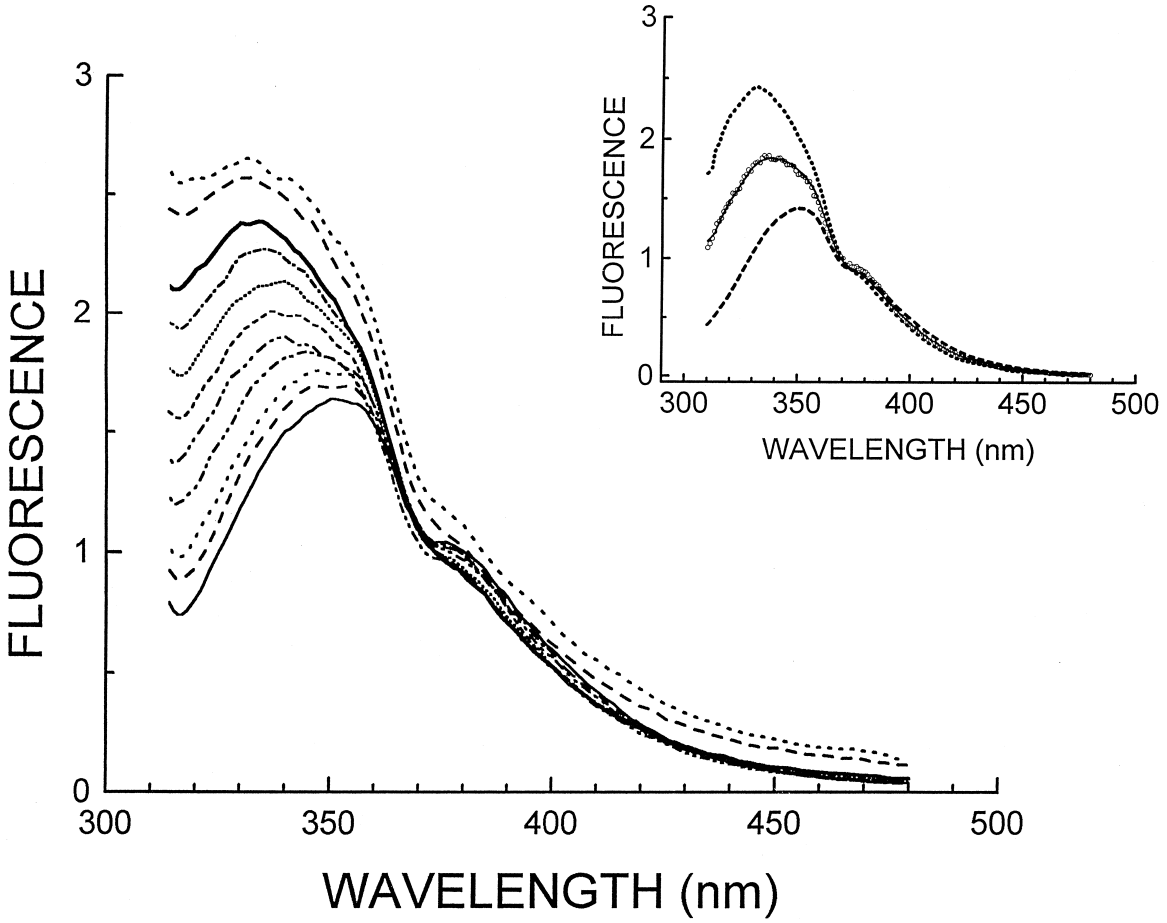

Fig. 2. Typical change in peptide (Ac-18A-NH_2, 12.5 μM) fluorescence spectra upon titration with vesicles (DOPC:DOPE, 1:1). From bottom to the top, lipid concentration is 0 μM, 6 μM, 12 μM, 25 μM, 38 μM, 50 μM, 62 μM, 87 μM, 145 μM, 290 μM, 460 μM. Background not subtracted. Difference between 145 μM, 290 μM and 460 μM spectra is only due to an increase in background fluorescence. Inset shows the fit of intermediate spectra by the sum of two components from bound and free peptide. Dashed and dotted lines are respectively the spectra of free and membrane bound peptide. Example of experimentally determined spectrum (lipid concentration 50 μM) is shown by open circles. Solid line shows the fit of the spectra by a linear combination of free and membrane bound spectra. Background signal was subtracted from all of the spectra.

We observed a significant difference between lipid and peptide titration assays. Values of bound peptide/lipid ratios at the same free peptide concentrations deduced from titration of liposomes with peptides were exactly two-fold less than those from the titration of peptide with vesicles. This can be explained by the different lipid accessibility in the two assays. Both 18L and Ac-18A-NH_2 peptides are able to permeabilize membranes at sufficiently high peptide/lipid ratios [11,12]. In the course of titration of peptide with vesicles the initially high free peptide concentrations led to the permeabilization of the first vesicles added, resulting in the accessibility of both sides of the membrane bilayer. Thus the bound peptide/lipid ratio is twice as high as in the titration of liposomes with peptide where the experiment starts with a low peptide-to-lipid ratio which is insufficient for vesicle disruption and thus only the outer vesicle surface is accessible.

We derived binding isotherms for 18L or Ac-18A-NH_2 with DOPC, DOPC:DOPE(1:1) or DOPG. Here we restricted our studies to lipids in the fluid phase since it was found previously that both Ac-18A-NH_2 and 18L do not penetrate into the gel phase [25,13]. The binding isotherm (Fig. 3) for 18L with all types of lipids appears linear until saturation at micromolar

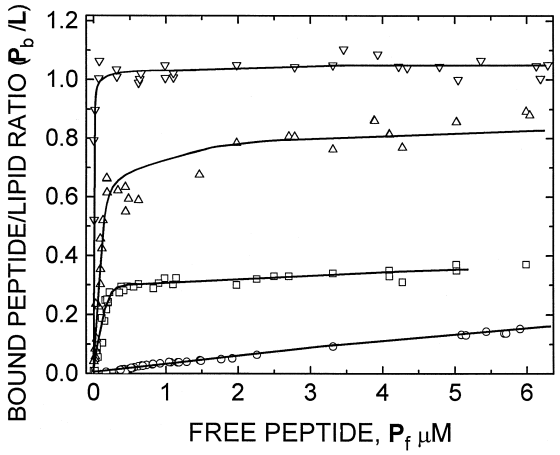

Fig. 3. Binding isotherms for 18L and Ac-18A-NH_2 peptides. The isotherm of binding of 18L to DOPG (∇), of Ac-18A-NH_2 for DOPG (Δ), of 18L to DOPC:DOPE (1:1) (□) and of Ac-18A-NH_2 to DOPC:DOPE (1:1) (○). Each binding isotherm was derived form several titration experiments as described in the text.

concentrations of free peptide. For Ac-18A-NH_2, such a pattern was observed only for acidic lipids. In the case of zwitterionic DOPC and DOPC:DOPE, no apparent saturation was observed. From the linear part of the binding isotherm, partition coefficients of peptide between water and the membrane phase, as well as the corresponding free energies of peptide–membrane association (ΔG_b), were determined (Table 1). Binding isotherms for DOPC and Ac-18A-NH_2 or 18L are not shown as they were similar to those of DOPC:DOPE. With less precision, Ac-18A-NH_2 or 18L binding to DMPC (at 37°C) and to DOPC:Chol (7:3) were also estimated and found similar to other zwitterionic lipids.

The proper resolution of the initial linear part of the binding isotherm and the determination of the binding constant requires titration of low peptide concentrations, such that P_0 is within the linear range of the isotherm $r(P_f)$. In practice this is limited by the need to have sufficient fluorescence signal above the background of the liposome suspensions, that is P_0 must be above $\sim 0.05\,\mu M$. This requirement corresponds to an upper limit of the binding constants (K) resolved by this assay of $K \sim 1/(5 \times 10^{-8}\,M) = 2 \times 10^7\,M^{-1}$ or a free energy of binding $\Delta G_b = -RT\ln(55.5 \times K) = -12.3$ kcal/mole (the cratic coefficient 55.5 M corresponds to the molar concentration of water which is invariant. It is included so as to make K dimensionless). For the stronger binding only the saturation part of the binding isotherm can be resolved. The range of K which can be determined by this assay is actually higher than that of a centrifugation assay [26], or a circular dichroism titration [27]. Measurement of the higher K can be achieved using fluorescently modified peptides.

The deconvolution procedure was modified for the quantitation of binding for peptides with very high membrane affinity, e.g. 18L:DOPG. If P_0 in the titration experiment is higher than the linear range of

Table 1
Equilibrium and dynamic parameters of the 18L and Ac-18A-NH_2 peptide binding with various types of lipids: association constants (K), free energy of association (ΔG_b), and association and dissociation rate constants (k_a and k_d)

Peptide	Lipid	Association constant, K, M^{-1}	[a]Free energy of association, $-\Delta G_b$, kcal/mol	[b]Association rate constant k_a, $M^{-1} \cdot s^{-1}$	[c]Dissociation rate constant k_d, s^{-1}
18L	DOPC:DOPE (1:1)	1.35×10^6	10.7	1.9×10^5	0.15
	DOPC	1.2×10^6	10.6	–	–
	DOPG	4.5×10^7	12.8	–	–
Ac-18A-NH_2	DOPC:DOPE (1:1)	3.2×10^4	8.5	1.3×10^5	3.9, 3.6[d]
	DOPC	4.0×10^4	8.6	–	–
	DOPG	3.5×10^6	11.3	2.8×10^5	0.075

[a] Free energy of peptide lipid association is calculated from the association constant K, as $\Delta G = -RT \cdot \ln(K \cdot 55.5)$.
[b] Association rate constants k_a were derived from the slope of the concentration dependence of association rate (Fig. 6).
[c] Dissociation rate constants k_d were calculated as $k_d = k_a/K$, except for [d] which was determined from concentration dependence of the association rate extrapolated to zero concentration.

the binding isotherm for that peptide/lipid system then the first liposome addition will lead to peptide binding with saturating peptide/lipid ratios and self-quenching of tryptophan fluorescence. An increase in the total fluorescence intensity is observed only when lipid is added to peptide which is already bound. This occurs without a significant change in the shape of the spectra. Eventually the fluorescence intensity reaches a maximum and a further addition of vesicles does not induce any changes after background subtraction. For quantitation of the peptide–membrane binding for these systems, the quenched bound peptide spectrum was used as a reference for the bound peptide and the same deconvolution procedure was applied. Comparing isotherms derived from several peptide concentrations we were able to resolve the saturation part of the binding isotherm. Only minimal estimates of K and ΔG_b are presented in Table 1 for the 18L:DOPG binding.

To examine the cooperativity of Ac-18A-NH_2 and 18L peptide membrane binding we derived isotherms of Ac-18A-NH_2 binding to vesicles preincubated with 18L at various peptide–lipid ratios. From the coincidence of this isotherms with the one without peptide preincubation, we conclude that the two peptides bind to membranes independently.

3.2. Kinetics of peptide binding

Increase in tryptophan fluorescence intensity (emission at 330 nm) was used to monitor the kinetics of peptide–membrane association. Association of both Ac-18A-NH_2 and 18L was found to be a fast process and to take place in tens of milliseconds. Typical time traces of peptide binding are presented (Fig. 4). The final extent of fluorescence increase depended on the lipid concentration for the Ac-18A-NH_2 peptide but was practically independent of lipid concentration for 18L. This was expected, since at the lipid concentrations used, according to the binding constants for DOPC:DOPE, the percentage of bound Ac-18A-NH_2 should depend on lipid concentration while 18L must always be essentially bound.

We fitted the time course of Ac-18A-NH_2 binding with a single first order rate constant. The plot of the binding rate constant versus lipid concentration is shown in Fig. 5. Such a distinct linear dependence is

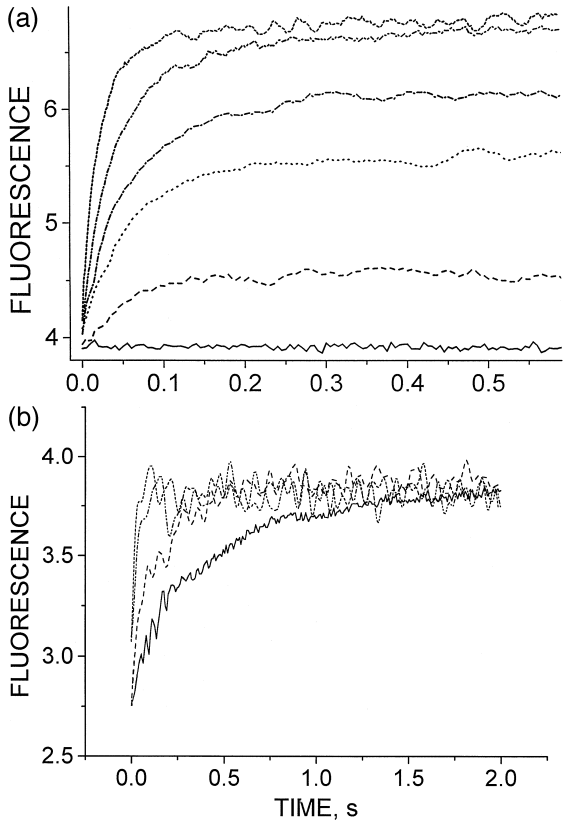

Fig. 4. Typical time course of peptide binding to membrane monitored by the increase of tryptophan fluorescence at 335 nm. (A) Kinetics of Ac-18A-NH_2 (5 μM) binding to DOPC:DOPE (1:1) LUV of the following concentrations: from the top to the bottom 340 μM, 170 μM, 85 μM, 50 μM, 25 μM, 0 μM. (B) Kinetics of 18L (5 μM) binding to DOPC:DOPE (1:1) LUV of the following concentrations: (from the left to the right) 250 μM, 200 μM, 50 μM, 32 μM. Experimental conditions are as described in Section 2.

characteristic of a one step association–dissociation equilibrium:

$$P_f + L \underset{k_d}{\overset{k_a}{\leftrightarrow}} P_b$$

Where P_f represents peptide in water, P_b the peptide associated with an aggregate of lipid molecules, L is an aggregate of lipid molecules, k_a – the rate constant of association and k_d – the rate constant of dissociation. In the case of excess lipid, the formally second order binding process follows pseudo first order kinetics, that is amount of the membrane bound peptide (P_b) approaches an equilibrium (P_{be}) following a single exponential time course with a rate constant R

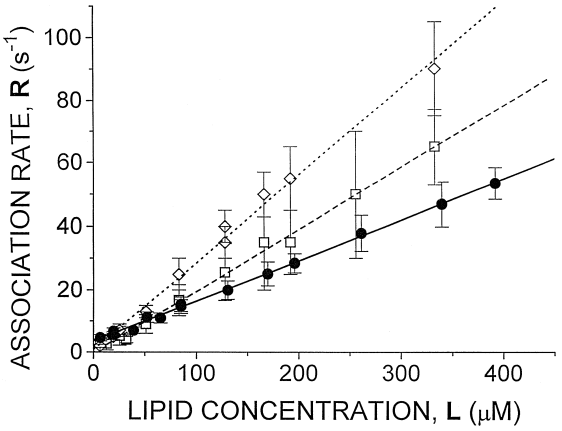

Fig. 5. Dependence of peptide binding rate constant (R), determined by monoexponential fit of the time traces, on lipid concentration (L). Straight lines are derived by linear regression. Circles and solid line - Ac-18A-NH_2 binding to DOPC:DOPE (1:1). Squares and dashed line - 18L binding to DOPC:DOPE (1:1). Diamonds and dotted line - Ac-18A-NH_2 binding to DOPG.

linearly dependent on lipid concentration (L):

$$P_b(t) = P_{be} \times (1 - \exp[-R \times t])$$

where

$$R = k_a \times L + k_d$$

For Ac-18A-NH_2 binding to DOPC:DOPE (Fig. 5) we calculate an association rate constant $k_a = 1.3 \times 10^5\,M^{-1}\,s^{-1}$ and a dissociation rate constant $k_d = 3.6 \pm 0.3\,s^{-1}$, which corresponds to a half-time of peptide dissociation $t_{1/2} = \ln(2)/k_d = 0.19 \pm 0.03$ s. Hence the corresponding equilibrium binding constant, $K = k_a/k_d = (3.5 \pm 0.3) \times 10^4\,M^{-1}$, is very close to the value of $K = 3.2 \times 10^4\,M^{-1}$ derived from the titration experiments (Table 1). To confirm the fast dynamic character of the Ac-18A-NH_2-membrane association equilibrium, we directly monitored the process of peptide dissociation from the membrane. Upon two fold dilution of the vesicle suspension preincubated with Ac-18A-NH_2, we observed partial peptide dissociation which was completed within 0.1–0.2 s (data not shown). In the case of high peptide/lipid ratios (> 1:20), the Ac-18A-NH_2 binding kinetics becomes more complicated. The initial rate increases above that expected from a linear dependence on concentration and the overall kinetics apparently becomes non-monoexponential and dependent both on peptide and lipid concentrations.

For the binding of 18L to the membrane, as well as Ac-18A-NH_2:DOPG binding, we were able to determine the peptide–membrane association rate constant k_a, but there was a large uncertainty in the determination of k_d. In addition to a monoexponential fit, association rates for these cases were analysed using an analytical expression for the kinetics of sequential binding [28,29] which takes into account saturation of binding. The values of the association rate constants derived by both approaches coincided within experimental error. Association rate constants are presented in Table 1.

Due to the high peptide-membrane affinity we were unable to directly determine the dissociation rate of 18L from DOPC:DOPE membranes, but we were able to confirm the dynamic character of the peptide–membrane equilibrium indirectly using the ANTS/DPX leakage assay (Fig. 6). A small aliquot of DOPG vesicles was added to 18L, which had been

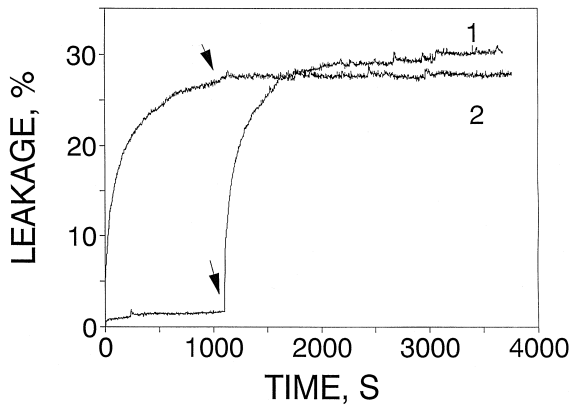

Fig. 6. Leakage experiment confirming the dynamic character of 18L partitioning between membranes. Curve 1: DOPC:DOPE (1:1) LUV (65 μM) were added to a solution of 3 μM 18L, causing relatively low leakage at this peptide/lipid ratio. At the arrow 15 μM of DOPC:DOPG (1:1) LUV were injected into the cell. Radistribution of 18L into these vesicles caused fast leakage. Curve 2: Control experiment, 15 μM of DOPC:DOPG LUV were injected into the cell with 5 μM 18L solution. The initial leakage rate is exactly the same as after DOPC:DOPG LUV injection in the Curve 1. At the arrow an additional 45 μM DOPC:DOPG LUV were injected which resulted in inhibition of leakage due to peptide redistribution and decrease of bound peptide/lipid ratios. 100% of leakage was determined by vesicle disruption with detergent and thus corresponds to the leakage of both DOPC:DOPE and DOPC:DOPG LUV in curve 1, and all DOPC:DOPG LUV in curve 2.

prebound to DOPC:DOPE vesicles at a non-leaky peptide/lipid ratio. The much higher affinity of 18L for acidic lipids results in the redistribution of 18L to acidic lipids and the induction of leakage. The pattern of leakage curves observed is similar to the one in the absence of zwitterionic liposomes (peptide in buffer), thus indicative of the peptide dissociation rate being faster than the leakage rate.

4. Discussion

4.1. Membrane partitioning

Binding isotherms $r(P_f)$ for both peptides, with all lipids studied, had a linear portion at low peptide/lipid ratios (Fig. 3). This linear part of the $r(P_f)$ corresponds to the peptide monomer partitioning into the membrane without subsequent aggregation [6]. Binding constants (K) have been derived from the slope of the linear part of the binding isotherms (Table 1). Binding constants of 18L are higher than those reported previously for similar peptides such as mastoparan ($K_{DOPC} = 1.65 \times 10^3\ M^{-1}$, [27]) or magainin 1 and 2 ($K_{DOPG} = 0.26 \times 10^6\ M^{-1}$; $3.0 \times 10^6\ M^{-1}$, [30]). Values of the binding constant for the Ac-18A-NH_2 peptide are also high compared to other data on membrane binding of analogs of A-type amphipathic peptides. In a recent paper, Spuhler et al. [26] report binding constants for the 18A (not the *N*-acetyl-peptide-amide, which we used in the present work), derived from a centrifugation assay, of $170\ M^{-1}$ for DOPC and $900\ M^{-1}$ for DOPC:DOPG, 1:1. The lower binding affinities of 18A compared to the Ac-18A-NH_2 are in accordance with the previously published observation that end group blockage of 18A significantly increases it's membrane affinity [14].

Binding isotherms show that the analysis using a partitioning model is valid only within a limited range of free peptide concentrations. With increased peptide–lipid ratios, the binding isotherm starts flattening and eventually goes to saturation. High membrane lytic activity of peptides necessitates the introduction of a coefficient of 0.5 for comparison of the vesicle and peptide titration experiments. The only exception to this was for Ac-18A-NH_2/DOPC:DOPE partitioning. In this case, the assumption that only the external leaflet of the membranes is available for peptide binding [31] was valid. The hyperbolic shape of the binding isotherms corresponds to the absence of in plane aggregation of peptides [6]. High peptide/lipid ratios in the binding isotherm give an estimate of the saturating bound peptide/lipid ratios: 1 for 18L and DOPG, 0.8 for Ac-18A-NH_2 and DOPG and 0.3 for 18L and DOPC:DOPE, which corresponds to one lipid molecule as the size of binding cluster in acidic lipid and three lipid molecules in DOPC:DOPE. Similar sizes of the 18L and Ac-18A-NH_2 binding clusters in acidic membranes suggest that it is determined primarily by steric (packing) considerations, while in zwitterionic membranes the limiting factor may be electrostatic repulsion of charged peptides. The very high saturation levels observed are indicative of vesicle disruption during the process of titration. This disruption could be monitored visually. Scattering (or turbidity) of vesicle suspension is dependent on the size of the vesicles. At sufficiently large peptide/lipid ratios, the 18L peptide increased the turbidity of both zwitterionic and acidic LUV which is indicative of aggregation and/or fusion of vesicles [12]. On the contrary Ac-18A-NH_2 peptide clarifies initially turbid MLV suspensions, which correlates with the known ability of class A peptide to solubilize membranes [14].

Binding of cationic peptides to zwitterionic and acidic membranes was previously described in terms of the Gouy-Chapman theory [31–33]. According to this description, negative charge on the acidic membrane creates a membrane potential which causes cationic peptides to redistribute to the membrane. This passive accumulation of peptides near an anionic membrane surface results in a high apparent binding constant. This aspect is important for the binding of cationic 18L. However, Ac-18A-NH_2 also had a much higher affinity for anionic membranes than for zwitterionic lipids (almost two orders of magnitude from DOPC to DOPG, Table 1). Titration calorimetry experiments show that the free energy of binding is of entropic origin both for 18L and Ac-18A-NH_2 and for both zwitterionic and acidic membranes (unpublished observation, Polozov et al.). Recently, it was found that the binding of the 18A peptide to the membrane does not change the overall surface charge of membranes [26], that is 18A is indeed zwitterionic in the membrane bound state. The

ratio of bound peptide to lipid for both 18L and Ac-18A-NH_2 at saturation was found to be higher for acidic lipids than for zwitterionic ones (Fig. 4). This also can not be explained only as a response to membrane potential. Rather, high peptide/lipid ratios at saturation are favoured by mutual repulsion of negatively charged lipid headgroups and also by reduction of peptide–peptide repulsion which may take place for the cationic 18L peptide. There also may be an input from the direct interaction of charged aminoacids with a charged lipid headgroups. Spuhler et al. [26] showed that 18A affects the conformation of lipid headgroups in a manner expected for positively charged peptides. This is consistent with the ''snorkel'' conformation adopted by 18A in a bilayer [14].

The monomer partitioning model is successful in describing the peptide binding kinetics as well as the equilibrium binding data. Peptides were found to be in dynamic equilibrium with membranes having an association time in the millisecond range and a dissociation speed which depended on the peptide affinity for membranes and ranged from hundreds of milliseconds to tens of seconds. The dynamic character of the binding equilibrium is highly lipid and peptide dependent. As it is shown in the Section 3, we derived an equilibrium binding constant, K, from experimentally determined association and dissociation rates of Ac-18A-NH_2 with DOPC:DOPE membranes and found it to coincide with the K derived from equilibrium studies. In accordance with the binding isotherm, we were not able to experimentally determine the dissociation rates for the 18L peptide or the Ac-18A-NH_2 peptide with acidic membranes. However, a knowledge of the association rate constant k_a, and the binding constant, K, are sufficient to completely describe the dynamic character of peptide binding. Variation in k_a was much less than that found for the equilibrium binding constant K. For example, k_a of Ac-18A-NH_2 for DOPG was only approximately two times higher than that for DOPC:DOPE, while the difference in K was three orders of magnitude. This shows that difference in peptide affinity for membranes, at least in the present case, is largely determined by the dissociation rate constant k_d as $k_d = k_a/K$. The upper boundary for the association rate constant is the diffusion limited rate constant, r_d.

It was shown theoretically [34] that:

$$r_d = b \times N_A \times D_0 \times (A_L/R_n)$$

involving b, the fraction of lipid molecules that are in the outer leaflet of the bilayer; N_A, Avogadro's number; D_0, the diffusion coefficient of the free peptide; A_L, the area per lipid headgroup on the bilayer surface; and R_n, the outer radius of a vesicle. For the DOPC:DOPE system we may estimate that $A_L = 0.7\,nm^2$, $R_n = 50\,nm$ and $b = 0.5$. The D_0 calculated for a peptide of about 2,000 MW at 25°C is $3 \times 10^{-6}\,cm^2/s$ [34]. Thus $r_d = 1.25 \times 10^6\,M^{-1}\,s^{-1}$ and the ratio $k_a/r_d = 0.104$ for association of Ac-18A-NH_2 with DOPC:DOPE. This shows that the measured association rates are relatively close to the diffusion limit, i.e. there is no large barrier for the entrance of a peptide molecule into the bilayer. It is thus understandable why variation in the binding constant occurs via the modulation of the dissociation rate constant. We can conclude that strong binding correlates with a slower exchange of peptide between water and membranes.

We found previously that activities of 18L and Ac-18A-NH_2 peptides depend strongly on the membrane composition, namely, on the presence of nonbilayer forming lipids and presence of acidic lipids [13]. Our current binding studies show that membrane charge strongly affects binding behavior of both cationic 18L and zwitterionic Ac-18A-NH_2. However, peptide binding was essentially not affected by the presence of nonbilayer forming lipids, that is, it was similar for several zwitterionic membranes studied.

4.2. Dynamic peptide–membrane equilibrium and peptide effects in biological systems

Certain L-type lytic peptides, originally extracted from amphibian skin [35,36], are suggested to protect the host from bacterial infection. From characterisation of the binding of 18L we can suggest that L-type peptides partition essentially complete into the membrane under ordinary conditions. Peptides are nonlytic for the host cells in vivo, due to the low peptide to total lipid ratio. However, due to the dynamic character of binding and the high peptide affinity for acidic membranes, the redistribution and accumulation of peptide at a lytic concentration on the acidic

membrane of bacteria may take place. We used 18L-induced vesicle contents leakage as a way to illustrate the dynamic character of peptide binding (Fig. 6). This data also shows the possibility of selective induction of leakage from acidic liposomes without affecting zwitterionic ones. At the same bound peptide/lipid ratios 18L is similarly lytic to both zwitterionic and acidic vesicles [13]. Thus the difference in membrane binding can explain why some L-type lytic peptides posses antibacterial activity at concentrations tolerant to the host cells. Due to the non-specific peptide–membrane binding, peptide antibiotic activity is expected to be pronounced at relatively high peptide concentrations. Increased specificity for binding to acidic membranes can serve as a guideline for the design of peptides for possible medical applications. Exposure of acidic lipids in malignant cells, can also serve as a method for targeting lytic peptides. This can explain the antitumor activity of magainins – L class peptide antibiotics [37]. Prebinding of peptides with liposomes can be used as a method for the reduction of acute toxicity upon peptide administration. The dynamic binding aspect of peptide action is not the only stage of regulation of peptide membrane permeabilization properties [38,39], but it is definitely an important stage in the regulation of peptide activities.

Acknowledgements

We would like to thank Dr. Julian G. Molotkovsky for providing the fluorescent lipid probes and Dr. Shlomo Nir for fruitful discussions.

References

[1] R.M. Epand, The Amphipathic Helix, CRC Press, Boca Raton, FL, 1993.
[2] G. Saberwal, N. Nagaraj, Biochim. Biophys. Acta 1197 (1994) 109–131.
[3] H. Duclohier, Toxicology 87 (1994) 175–188.
[4] G. Schwarz, H. Gerke, V. Rizzo, S. Stankowski, Biophys. J. 52 (1987) 685–692.
[5] G. Schwarz, G. Beschiaschvili, Biochim. Biophys. Acta 979 (1989) 82–90.
[6] G. Schwarz, Biochimie 71 (1989) 1–9.
[7] K.M. Sekharam, T.D. Bradrick, S. Georghiou, Biochim. Biophys. Acta 1063 (1991) 171–174.
[8] T.D. Bradrick, A. Philippetis, S. Georghiou, Biophys. J. 69 (1995) 1999–2011.
[9] C. Golding, S. Senior, M.T. Wilson, P. O'Shea, Biochemistry 35 (1996) 10931–10937.
[10] J.P. Segrest, H. De Loof, J.G. Dohlman, C.G. Brouilette, G.M. Anantharamaiah, Proteins 8 (1990) 103–117.
[11] E.M. Tytler, J.P. Segrest, R.M. Epand, S.-Q. Nie, R.F. Epand, V.K. Mishra, Y.V. Venkatachalapathi, G.M. Anantharamaiah, J. Biol. Chem. 268 (1993) 22112–22118.
[12] I.V. Polozov, A.I. Polozova, E.M. Tytler, G.M. Anantharamaiah, J.P. Segrest, G.A. Wooley, R.M. Epand, Biochemistry 36 (1997) 9237–9245.
[13] I.V. Polozov, A.I. Polozova, J.G. Molotkovsky, R.M. Epand, Biochim. Biophys. Acta 1328 (1997) 125–139.
[14] Y.V. Venkatachalapathi, M.C. Phillips, R.M. Epand, R.F. Epand, E.M. Tytler, J.P. Segrest, G.M. Anantharamaiah, Proteins 15 (1993) 349–359.
[15] G.M. Anantharamaiah, Methods Enzymol. 128 (1986) 627–647.
[16] V.K. Mishra, M.N. Palgunachari, J.P. Segrest, G.M. Anantharamaiah, J. Biol. Chem. 269 (1994) 7185–7191.
[17] B.N. Ames, Methods Enzymol. 8 (1966) 115–118.
[18] M. Smolarsky, D. Teitelbaum, M. Sela, C. Gitler, J. Immunol. Methods 15 (1977) 255–265.
[19] I.V. Polozov, A.I. Polozova, G.M. Anantharamaiah, J.P. Segrest, R.M. Epand, Biochem. Mol. Biol. Int. 33 (1994) 1073–1079.
[20] H. Ellens, J. Bentz, F.C. Szoka, Biochemistry 23 (1984) 1532–1538.
[21] J.P. Segrest, B.H. Chung, C.G. Brouillette, P. Kanellis, R. McGan, J. Biol. Chem. 258 (1983) 2290–2295.
[22] H.J. Pownall, A.M. Gotto Jr., J. Sparrow, Biochim. Biophys. Acta 793 (1984) 149–156.
[23] R.M. Epand, R.F. Epand, Biochim. Biophys. Acta 602 (1980) 600–609.
[24] K. Matsuzaki, O. Murase, H. Tokuda, S. Funakoshi, N. Fujii, K. Miyajima, Biochemistry 33 (1994) 3342–3349.
[25] I.V. Polozov, A.I. Polozova, J.G. Molotkovsky, G.M. Anantharamaiah, J.P. Segrest, R.M. Epand, Biophys. J. 68 (1995) A433.
[26] P. Spuhler, G.M. Anantharamaiah, J.P. Segrest, J. Seelig, J. Biol. Chem. 269 (1994) 23904–23910.
[27] G. Schwarz, U. Blochman, FEBS Lett. 318 (1993) 172–176.
[28] J. Bentz, S. Nir, D. Covell, Biophys. J. 54 (1988) 449–462.
[29] S. Nir, R. Peled, K.-D. Lee, Colloids and Surfaces A 89 (1994) 45–57.
[30] K. Matsuzaki, M. Harada, S. Funakoshi, N. Fujii, K. Miyajima, Biochim. Biophys. Acta 1063 (1991) 162–170.
[31] G. Beschiashchvili, J. Seelig, Biochemistry 29 (1990) 52–58.
[32] E. Kuchinka, J. Seelig, Biochemistry 28 (1989) 4216–4221.
[33] M. Mosior, S. McLaughlin, Biochim. Biophys. Acta 1105 (1992) 185–187.
[34] G. Schwarz, Biophys. Chem. 26 (1987) 163–169.
[35] M. Zasloff, Proc. Natl. Acad. Sci. U.S.A. 84 (1987) 5449–5453.

[36] M. Zasloff, B. Martin, H.-C. Chen, Proc. Natl. Acad. Sci. U.S.A. 85 (1988) 910–913.
[37] R.A. Cruciani, J.L. Barker, M. Zasloff, H.-C. Chen, O. Colamonici, Proc. Natl. Acad. Sci. U.S.A. 88 (1991) 3792–3796.
[38] K. Matsuzaki, K.-L. Sugishita, N. Fujii, K. Miyajima, Biochemistry 34 (1995) 3423–3429.
[39] E.M. Tytler, G.M. Anantharamaiah, D.E. Walker, V.K. Mishra, M.N. Palgunachari, J.P. Segrest, Biochemistry 34 (1995) 4393–4401.